

# Truncation effects in superdiffusive front propagation with Lévy flights

D. del-Castillo-Negrete

Oak Ridge National Laboratory, Oak Ridge, Tennessee 37831-8071, USA

(Received 18 December 2008; published 26 March 2009)

A numerical and analytical study of the role of exponentially truncated Lévy flights in the superdiffusive propagation of fronts in reaction-diffusion systems is presented. The study is based on a variation of the Fisher-Kolmogorov equation where the diffusion operator is replaced by a  $\lambda$ -truncated fractional derivative of order  $\alpha$ , where  $1/\lambda$  is the characteristic truncation length scale. For  $\lambda=0$  there is no truncation, and fronts exhibit exponential acceleration and algebraically decaying tails. It is shown that for  $\lambda \neq 0$  this phenomenology prevails in the intermediate asymptotic regime  $(\chi t)^{1/\alpha} \ll x \ll 1/\lambda$  where  $\chi$  is the diffusion constant. Outside the intermediate asymptotic regime, i.e., for  $x > 1/\lambda$ , the tail of the front exhibits the tempered decay  $\phi \sim e^{-\lambda x/x^{(1+\alpha)}}$ , the acceleration is transient, and the front velocity  $v_L$  approaches the terminal speed  $v_* = (\gamma - \lambda^\alpha \chi)/\lambda$  as  $t \rightarrow \infty$ , where it is assumed that  $\gamma > \lambda^\alpha \chi$  with  $\gamma$  denoting the growth rate of the reaction kinetics. However, the convergence of this process is algebraic,  $v_L \sim v_* - \alpha/(\lambda t)$ , which is very slow compared to the exponential convergence observed in the diffusive (Gaussian) case. An overtruncated regime in which the characteristic truncation length scale is shorter than the length scale of the decay of the initial condition,  $1/\nu$ , is also identified. In this extreme regime, fronts exhibit exponential tails,  $\phi \sim e^{-\nu x}$ , and move at the constant velocity  $v = (\gamma - \lambda^\alpha \chi)/\nu$ .

DOI: 10.1103/PhysRevE.79.031120

PACS number(s): 02.50.Ey, 82.40.Ck, 05.40.Fb

## I. INTRODUCTION

Reaction-diffusion systems have played a predominant role in the study of pattern formation and nonlinear dynamics in a large class of phenomena of interest to physics, biology, chemistry, and engineering; see, for example, Refs. [1,2], and references therein. One of the simplest reaction-diffusion systems is the extensively studied Fisher-Kolmogorov model that describes the dynamics of a scalar field  $\phi$  in a one-dimensional domain,

$$\partial_t \phi = \chi \partial_x^2 \phi + \gamma \phi(1 - \phi), \quad (1)$$

where  $\chi$  denotes the diffusivity and  $\gamma$  is a constant. The nontrivial dynamics of reaction-diffusion systems in general stems from the competition between the diffusivity and the nonlinearity. In the case of the Fisher-Kolmogorov equation this competition leads to the propagation of fronts in which the stable,  $\phi=1$ , state advances through the destabilization of the  $\phi=0$  unstable state.

An important and often overlooked assumption in reaction-diffusion models is the use of Laplacian operators  $\chi \nabla^2$  for the description of transport. The use of these operators is motivated by the Fourier-Fick model according to which the flux  $q$  is assumed to be proportional to the gradient of the concentration,  $\mathbf{q} = -\chi \nabla \phi$ . This local prescription, together with the conservation law  $\partial_t \phi = -\nabla \cdot \mathbf{q}$ , leads to the Laplacian, diffusive transport operator. From the statistical mechanics point of view this prescription is linked to the assumption that the underlying “microscopic” transport process is driven by an uncorrelated, Markovian, Gaussian process. However, despite its relative success, experimental, numerical, and theoretical evidence indicates that the diffusion model has limited applicability; see, for example, Refs. [3–6], and references therein. Therefore, a problem of considerable interest is the study of the role of anomalous diffusion, and Lévy flights in particular, in reaction-diffusion systems.

Early work on reaction–anomalous-diffusion systems include Refs. [7–10]. Reference [7] studied bistable reaction processes and anomalous diffusion caused by Lévy flights. The interplay of subdiffusion and Turing instabilities was discussed in Ref. [8]. The role of superdiffusive transport in the acceleration and algebraic decay of fronts was studied in the context of a probabilistic approach in Ref. [9] and in the context of an equivalent fractional Fisher-Kolmogorov equation in Ref. [10]. It is interesting to note that fronts in chaotic coupled-map lattices with long-range couplings exhibit an analogous phenomenology as discussed in Ref. [11]. More recent works include the study of analytic solutions of fractional reaction diffusion [12]; the study of a reaction-diffusion system with a bistable reaction term and directional anomalous diffusion [13]; the study of the construction of reaction-subdiffusion equations [14]; the study of Turing instabilities [16]; the study of the effect of superdiffusion on pattern formation selection in the Brusselator model [17]; and the study of the fractional Ginzburg-Landau and Kuramoto-Sivashinsky equations [18], among others.

Evidence of Lévy flights has been found in laboratory experiments, simple models, and numerical studies of turbulent transport, and the use of fractional diffusion models to describe these problems has been well documented in the literature [5]. However, it is plausible that finite-size domain and decorrelation effects (among other effects) might have an impact on the Lévy flight dynamics. The evaluation of the role of these “nonideal” effects on reaction–anomalous-diffusion systems is a problem of considerable practical relevance. Of particular importance is to determine how, and to what degree, these effects might mask the underlying Lévy statistics. The effect of fluctuations caused by finite number of particles per volume on the superdiffusive propagation of fronts was studied in Ref. [15]. Here we focus on the role of truncation effects on Lévy flights driving superdiffusive front propagation.

Asymptotic analysis plays an important role in the evaluation of nonideal Lévy flight effects. In particular, it is quite

possible that because of nonideal effects the statistics of the system will eventually converge to Gaussian. However, the key issue is to determine the duration of the nondiffusive transient and the rate of convergence to Gaussian statistics. This point is clearly illustrated in the ultraslow convergence to Gaussian statistics in the presence of truncated Lévy flights. In this case it has been observed that although the statistics eventually converges to Gaussian (because of the central limit theorem) a remarkably large number of steps is needed, and therefore the system effectively behaves nondiffusively in the intermediate asymptotic regime of practical interest [19–23]. In the present paper we explore to what degree a similar situation occurs in the case of front propagation. In particular, in Ref. [10] it was shown that in the fractional Fisher-Kolmogorov equation fronts decay algebraically and exhibit exponential acceleration. The goal of this paper is to present a numerical and analytical asymptotic study of the effect of truncation on these phenomena. One problem of special interest is to determine if there is an intermediate asymptotic regime where the effects of truncation are negligible and where the fronts accelerate and exhibit algebraic tails. Outside such intermediate asymptotic regime it is expected that the truncation effects will become dominant and that as  $t \rightarrow \infty$  the front dynamics will eventually approach in some sense the diffusive Fisher-Kolmogorov dynamics. However, the key issue is how long this will take. This brings us to the second problem of interest in this paper, which is to determine the rate of convergence to the constant velocity and exponential tails characteristic of the diffusive front propagation regime.

Our approach is based on the use of truncated fractional diffusion operators. Fractional derivatives provide a powerful framework to model nondiffusive transport processes [6,5]. These operators incorporate long-range, nonlocal transport through the use of slowly decaying kernels. In particular, in fractional diffusion the Laplacian is replaced by an integral operator of the form  $\partial_x^2 \int \phi(x', t) K(x-x') dx'$ , where the kernel  $K$  has the asymptotic behavior,  $K \sim x^{-\alpha+1}$ , for  $1 < \alpha < 2$ . In the context of the continuous time random walk model the exponent  $\alpha$  is related to the stability index of the underlying Lévy process [6]. However, a potential drawback of this description is that  $\alpha$ -stable Lévy processes have divergent second moments because their corresponding densities decay as  $\sim x^{-(1+\alpha)}$ . This issue has motivated the consideration of truncated Lévy processes that exhibit long-range dynamics while preserving the finiteness of some [24] or all moments [19,20,23]. In the case of exponentially truncated processes, the Lévy density decays as  $\sim x^{-(1+\alpha)} e^{-\lambda x}$ , and for  $\lambda \neq 0$  all the moments are finite. In the present paper we limit attention to this type of process and study the truncated fractional Fisher-Kolmogorov in which the Laplacian operator in Eq. (1) is replaced by the truncated fractional diffusion operator proposed in Ref. [23].

The organization of the rest of the paper is as follows. The next section reviews material on truncated Lévy flights, defines the  $\lambda$ -truncated fractional derivatives, and discusses the fundamental solutions and scaling properties of the truncated fractional diffusion equation. Section III contains the core of the numerical results obtained from the integration of the truncated fractional Fisher-Kolmogorov equation for front-

type initial conditions. Section IV presents an analytical asymptotic study based on the leading edge approximation. The conclusions are presented in Sec. V.

## II. FRACTIONAL DIFFUSION WITH TRUNCATED LÉVY FLIGHTS

In the standard fractional diffusion model the transport of a scalar  $\phi$  is governed by the equation

$${}^c D_t^\beta \phi(x,t) = -a \partial_x \phi + c(l {}_{L-\infty} D_x^\alpha + r {}_x D_\infty^\alpha) \phi, \quad (2)$$

where we have included in addition to the spatial and temporal fractional operator an advective term. The operator on the left-hand side is the regularized (in the Caputo sense [25]) fractional time derivative

$${}^c D_t^\beta \phi = \frac{1}{\Gamma(1-\beta)} \int_0^t \frac{\partial_\tau \phi}{(t-\tau)^\beta} d\tau, \quad (3)$$

with  $0 < \beta < 1$ , and the operators on the right-hand side of Eq. (2) are the left and right Riemann-Liouville fractional derivatives [25,26]

$$D_x^\alpha \phi = \frac{1}{\Gamma(m-\alpha)} \frac{\partial^m}{\partial x^m} \int_a^x \frac{\phi}{(x-y)^{\alpha+1-m}} dy, \quad (4)$$

$$D_b^\alpha \phi = \frac{(-1)^m}{\Gamma(m-\alpha)} \frac{\partial^m}{\partial x^m} \int_x^b \frac{\phi}{(y-x)^{\alpha+1-m}} dy, \quad (5)$$

with  $m-1 \leq \alpha < m$ . The weighting factors  $l$  and  $r$  are defined as

$$l = -\frac{(1-\theta)}{2 \cos(\alpha\pi/2)}, \quad r = -\frac{(1+\theta)}{2 \cos(\alpha\pi/2)}, \quad (6)$$

with  $-1 < \theta < 1$ . According to Eqs. (2) and (6), the parameter  $\theta$  determines the degree of asymmetry of the fractional operator. For  $\theta=0$  the contributions of left and right derivatives are equal and the operator is symmetric. In the extremal, fully asymmetric case of main interest in this paper,  $\theta=-1$ , and only the left derivative is present in the diffusion operator. Equation (2) describes the fluid limit of a continuous time random walk (CTRW) in the case when the waiting time distribution function exhibits algebraic decay of the form,  $\psi \sim t^{-1-\beta}$ , and the particle jumps follow an  $\alpha$ -stable Lévy distribution; see, for example, [6], and references therein.

The fractional equation (2) has found applications in several areas of physics, engineering, and biology. For a recent discussion on the basic theory and applications of fractional diffusion, see [5]. However, more general transport equations can be obtained when a wider class of stochastic processes are considered. In particular, in the case when the particle jump probability density function corresponds to an exponentially truncated (tempered) distribution with characteristic exponent of the form [20]

$$\Lambda_{\text{ET}} = iak - \frac{c}{2 \cos(\alpha\pi/2)} \times \begin{cases} (1 + \theta)(\lambda + ik)^\alpha + (1 - \theta)(\lambda - ik)^\alpha - 2\lambda^\alpha, \\ (1 + \theta)(\lambda + ik)^\alpha + (1 - \theta)(\lambda - ik)^\alpha - 2\lambda^\alpha \\ - 2ik\alpha\theta\lambda^{\alpha-1}, \end{cases} \quad (7)$$

for  $0 < \alpha < 1$  and  $1 < \alpha \leq 2$ , respectively. The fluid limit of the corresponding CTRW leads to the equation [23]

$${}^c D_t^\beta \phi = -V \partial_x \phi + c D_x^{\alpha,\lambda} \phi - \mu \phi, \quad (8)$$

where the  $\lambda$ -truncated fractional derivative operator of order  $\alpha$ ,  $D_x^{\alpha,\lambda}$ , is defined as

$$D_x^{\alpha,\lambda} = l e^{-\lambda x} D_x^\alpha e^{\lambda x} + r e^{\lambda x} D_x^\alpha e^{-\lambda x}. \quad (9)$$

The effective advection velocity is  $V=a$  for  $0 < \alpha < 1$  and  $V=a-v$  for  $1 < \alpha < 2$  with

$$v = \frac{c\alpha\theta\lambda^{\alpha-1}}{|\cos(\alpha\pi/2)|} \quad (10)$$

and

$$\mu = -\frac{c\lambda^\alpha}{\cos(\alpha\pi/2)}. \quad (11)$$

According to Eq. (10), in the case  $1 < \alpha < 2$ , the truncation gives rise to a drift that depends on the asymmetry of the process. The parameter  $\lambda$  determines the truncation of the tempered Lévy process whose corresponding Lévy density is given by [20]

$$w_{\text{ET}}(x) = \begin{cases} c \frac{(1 + \theta)}{2} |x|^{-(1+\alpha)} e^{-\lambda|x|} & \text{for } x < 0, \\ c \frac{(1 - \theta)}{2} x^{-(1+\alpha)} e^{-\lambda x} & \text{for } x > 0, \end{cases} \quad (12)$$

$0 < \alpha \leq 2$ ,  $c > 0$ ,  $-1 \leq \theta \leq 1$ , and  $\lambda \geq 0$ . As expected, for  $\lambda = 0$ , Eq. (12) reduces to the  $\alpha$ -stable density, and Eq. (8) reduces to Eq. (2).

The general solution of Eq. (8) for an initial condition  $\phi(x, t=0) = \phi(x, 0)$  is

$$\phi(x, t) = \int_{-\infty}^{\infty} G_{\alpha,\beta,\theta,\lambda}(x - x', t) \phi(x', 0) dx', \quad (13)$$

where  $G_{\alpha,\beta,\theta,\lambda}$  is the Green's function or propagator which corresponds to the solution with initial condition  $\phi(x, t=0) = \delta(x)$ . The subscripts of  $G$  state explicitly that in general the solution depends on four parameters: the order of the fractional derivative in space  $\alpha$ , the order of the fractional time derivative  $\beta$ , the asymmetry of the fractional operator  $\theta$ , and the truncation  $\lambda$ . Using the Fourier transform properties of the truncated fractional derivative it follows that

$$G_{\alpha,\beta,\theta,\lambda}(x, t) = \frac{1}{2\pi} \int_{-\infty}^{\infty} e^{-ikx} E_\beta[t^\beta \Lambda_{\text{ET}}(k)] dk, \quad (14)$$

where  $E_\beta$  denotes the Mittag-Leffler function and  $\Lambda_{\text{ET}}$  is given in Eq. (7). At first sight the linear term,  $-\mu\phi$ , on the right-hand side of Eq. (8) seems strange and likely to give

rise to an unphysical damping of the transported field  $\phi$ . However, quite to the contrary, this term is critical to guarantee the conservation of  $\phi$ . When  $\phi$  is interpreted as a probability density function, this term guarantees the normalization and conservation of the total probability. One way to see this is to note that this term comes from the term proportional to  $-2\lambda^\alpha$  in (7), which implies  $\Lambda_{\text{ET}}(k=0) = 0$ . According to Eqs. (13) and (14)  $\int \phi(x, t) dx = E_\beta[t^\beta \Lambda_{\text{ET}}(k=0)] \int \phi_0(x) dx$  which guarantees the conservation of  $\phi$  provide  $\Lambda_{\text{ET}}(k=0) = 0$ , since  $E_\beta(0) = 1$ .

In this paper we focus on the special case of Eq. (8) with  $1 < \alpha < 2$ ,  $\beta = 1$ , and  $\theta = -1$ . Also, we assume an advection velocity  $a = v$ , which results in the following asymmetric, truncated fractional equation:

$$\partial_t \phi = \chi [e^{-\lambda x} D_x^\alpha (e^{\lambda x} \phi) - \lambda^\alpha \phi], \quad (15)$$

with  $\chi = c/|\cos(\alpha\pi/2)|$ . We restrict attention to this special case because it corresponds to the truncated version of the  $\alpha$ -stable asymmetric fractional operator used in the front acceleration problem discussed in Ref. [10]. For this case, the general solution in Eq. (14) reduces to

$$G_{\alpha,1,-1,\lambda} = \frac{1}{2\pi} \int_{-\infty}^{\infty} e^{-ikx + \chi t [(\lambda - ik)^\alpha - \lambda^\alpha]} dk, \quad (16)$$

which can be equivalently written as

$$G_{\alpha,1,-1,\lambda} = e^{-\lambda x - \chi \lambda^\alpha t} (\chi t)^{-1/\alpha} \hat{G}_{\alpha,1,-1,0}(\eta), \quad (17)$$

where

$$\hat{G}_{\alpha,1,-1,0}(\eta) = \frac{1}{2\pi} \int_{-\infty}^{\infty} e^{i\alpha k^\alpha + ik\eta} dk \quad (18)$$

is the Green's function of the asymmetric,  $\alpha$ -stable ( $\lambda = 0$ ) fractional diffusion equation, in terms of the similarity variable  $\eta = x(\chi t)^{-1/\alpha}$ . From here, using the asymptotic expression,  $\hat{G}_{\alpha,1,-1,0}(\eta) \sim \eta^{-1-\alpha}$  for  $\eta > 0$  [27,28] it follows that

$$G_{\alpha,1,-1,\lambda} \sim \chi t e^{-\chi \lambda^\alpha t} \frac{e^{-\lambda x}}{x^{1+\alpha}}, \quad (19)$$

for  $x > 0$  and  $x \gg (\chi t)^{1/\alpha}$ . For the decay of the left tail, we use the asymptotic expansion  $\hat{G}_{\alpha,1,-1,0}(\eta) \sim |\eta|^{a_2} e^{-b_2 |\eta|^{c_2}}$  for  $\eta < 0$  and  $|\eta| \gg 1$ , where  $a_2 = (2 - \alpha)/[2(\alpha - 1)]$ ,  $b_2 = (\alpha - 1)\alpha^{\alpha/(\alpha-1)}$ , and  $c_2 = \alpha/(\alpha - 1)$  [28], to conclude

$$G_{\alpha,1,-1,\lambda} \sim (\chi t)^{-(a_2+1)/\alpha} e^{-\chi \lambda^\alpha t} |x|^{a_2} e^{-b_2 (\chi t)^{-c_2/\alpha} |x|^{c_2 + \lambda|x|}} \quad (20)$$

for  $x < 0$  and  $|x| \gg (\chi t)^{1/\alpha}$ . Since we are assuming that  $1 < \alpha < 2$ , it follows that  $c_2 > 1$  and the  $-|x|^{c_2}$  term in the exponent dominates the  $\lambda|x|$  term, leading to a faster than exponential decay of the left tail for any value of  $\lambda$ . Figure 1 shows plots of the Green's function in Eq. (16) for  $\alpha = 1.5$  and different values of  $\lambda$ , along with the asymptotic approximation in Eq. (19).

An important property of truncated Lévy flights, originally discussed in Refs. [19,21,22], is the ultraslow convergence to Gaussian statistics. According to this result, the crossover time for Gaussian behavior to appear,  $\tau_c$ , scales as

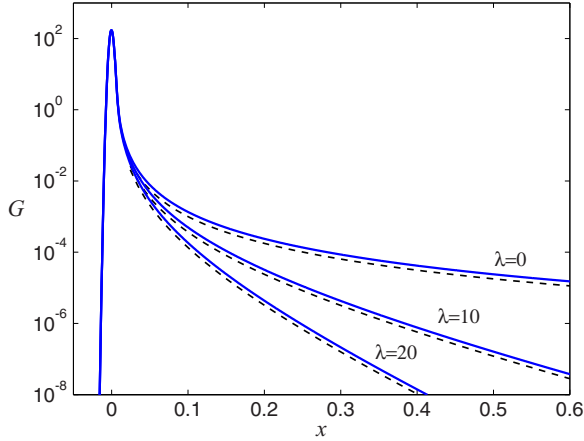


FIG. 1. (Color online) Green's functions of the asymmetric truncated fractional diffusion Eq. (16) for  $\alpha=1.5$ ,  $\theta=-1$ , and  $\lambda=0, 10$ , and  $20$ . The solid (blue) lines show  $G$  as a function of  $x$  for fixed  $t$ , and the dashed (black) lines show the corresponding asymptotic dependence according to Eq. (19). The numerical and asymptotic results are practically indistinguishable for  $x>0.1$ , and for visualization purposes the asymptotic result has been shifted downward a little in the plot.

$$\tau_c \sim \chi^{-1} \lambda^{-\alpha}, \quad (21)$$

as expected, as  $\lambda \rightarrow 0$ ,  $\tau \rightarrow \infty$ . When memory effects are incorporated using fractional time derivatives, the crossover dynamics is richer. In particular, for  $2\beta/\alpha > 1$ ,  $\tau_c \sim \chi^{-1/\beta} \lambda^{-\alpha/\beta}$  signals the crossover from superdiffusive to subdiffusive dynamics [23]. The time scale  $\tau_c$  will play an important role in the dynamics of the fronts.

### III. FRONT PROPAGATION IN THE PRESENCE OF TRUNCATED LÉVY FLIGHTS: NUMERICAL RESULTS

To study the role of truncation in the superdiffusive acceleration of fronts due to Lévy flights we consider the fractional Fisher-Kolmogorov equation originally introduced in Ref. [10] and substitute the Riemann-Liouville fractional derivatives (which correspond to  $\alpha$ -stable Lévy processes) by the truncated fractional derivative in Eq. (9). In the most general case the resulting equation is

$${}_0^c D_t^\beta \phi = -V \partial_x \phi + c \mathcal{D}_x^{\alpha, \lambda} \phi - \mu \phi + \gamma \phi(1 - \phi). \quad (22)$$

However, as mentioned before, to compare the results with those in Ref. [10] we will restrict attention to asymmetric, truncated fractional diffusion operators of the form in Eq. (15) and consider

$$\partial_t \phi = \chi [e^{-\lambda x} {}_{-\infty}^c D_x^\alpha (e^{\lambda x} \phi) - \lambda^\alpha \phi] + \gamma \phi(1 - \phi). \quad (23)$$

In this section we present results obtained from the numerical integration of Eq. (23). We assume  $\phi=A$ , for  $x<0$ , where  $A$  is a constant and discretize the fractional derivative in the  $x \in (0, 1)$  domain using the Grunwald-Letnikov representation. Details of finite-difference methods for the solution of fractional diffusion equations can be found in [29,30]. In all the numerical simulations we consider  $\alpha=1.5$ ,  $\theta=-1$ ,  $\gamma=1$ ,  $\chi=5 \times 10^{-7}$ , and initial conditions of the form

$$\phi(x, t=0) = e^{-\nu x}, \quad (24)$$

where  $\nu$  is a constant.

Figure 2(a) shows snapshots of the front profile  $\phi$  as function of  $x$  at different times in the  $\alpha$ -stable ( $\lambda=0$ ) case obtained from the numerical solution of Eq. (23). In this case the front exhibits an algebraically decaying tail which in log-log scale manifests as a straight line [10]. Figure 2(b) shows that the algebraic decay of the tail remains for small values of  $\lambda$ . In fact, as we will discuss in the next section, there is an intermediate asymptotic regime in which the role of truncation is negligible. Outside the intermediate asymptotic regime the effect of the truncation depends critically on the ratio of the length scale of the truncation,  $1/\lambda$ , and length scale  $1/\nu$  of the initial condition. When,  $\lambda < \nu$ , i.e., when the initial condition decays faster than the truncation, the tail of the front scales as  $\phi \sim x^{-1-\alpha} e^{-\lambda x}$  as shown in Fig. 2(c). On the other hand, when  $\lambda > \nu$ , the truncation effects dominate and Lévy statistics seems to have no effect on the dynamics of the front which, as shown in Fig. 2(d) (note the log-normal scale), exhibits the usual exponential decay of the diffusive Fisher-Kolmogorov model.

When the front exhibits “rigid” propagation with a constant velocity, as in the diffusive Fisher-Kolmogorov case, it is straightforward to define and numerically compute the front speed. However, when the front accelerates and deforms, as is the case in the  $\alpha$ -stable and truncated fractional Fisher-Kolmogorov equation, computing the front speed is not straightforward. One way to approach this problem is to consider the Lagrangian trajectory of the front's tail. For a given value of  $\phi_0$ , we define the Lagrangian trajectory,  $x_L = x_L(t)$ , of the front according to  $\phi(x_L(t), t) = \phi_0$ . Given  $x_L$  we define the Lagrangian velocity as  $v_L = dx_L/dt$  and the Lagrangian acceleration as  $a_L = dv_L/dt$ .

Figure 3 shows space-time plots of the Lagrangian trajectories of fronts corresponding to  $\phi_0=10^{-6}$ . Due to the relatively small value of  $\phi_0$ , these orbits follow the Lagrangian dynamics of the fronts' leading edge. The solid lines denote the numerical values for different values of  $\lambda$  and the dashed lines denote the result of the asymptotic analytic calculation that will be discussed in the next section. For  $0 \leq \lambda < 1$  it is observed that the front propagates very fast. However, as  $\lambda$  increases the speed of the front is reduced. The corresponding Lagrangian velocities and accelerations are shown in Figs. 4 and 5. For small  $\lambda$ , the front acceleration grows monotonically. However, for larger values of  $\lambda$  the Lagrangian velocity approaches a terminal velocity as  $t \rightarrow \infty$ . Note that as  $\lambda$  increases, the terminal velocity is smaller and the convergence is faster.

As shown in Fig. 5, in all cases the acceleration exhibits a pulselike behavior in the time evolution. The time of peaking of the pulse increases (approximately exponentially) with  $\lambda$  and the amplitude of the acceleration's peak decreases (approximately exponentially) with  $\lambda$ . However, the key feature to note is the evolution of the acceleration following the transient short pulse. For small  $\lambda$  the front acceleration exhibits a monotonic increase whereas for larger values the acceleration exhibits a transient growth followed by an eventual decay. Figure 6 shows the asymptotic scaling behavior

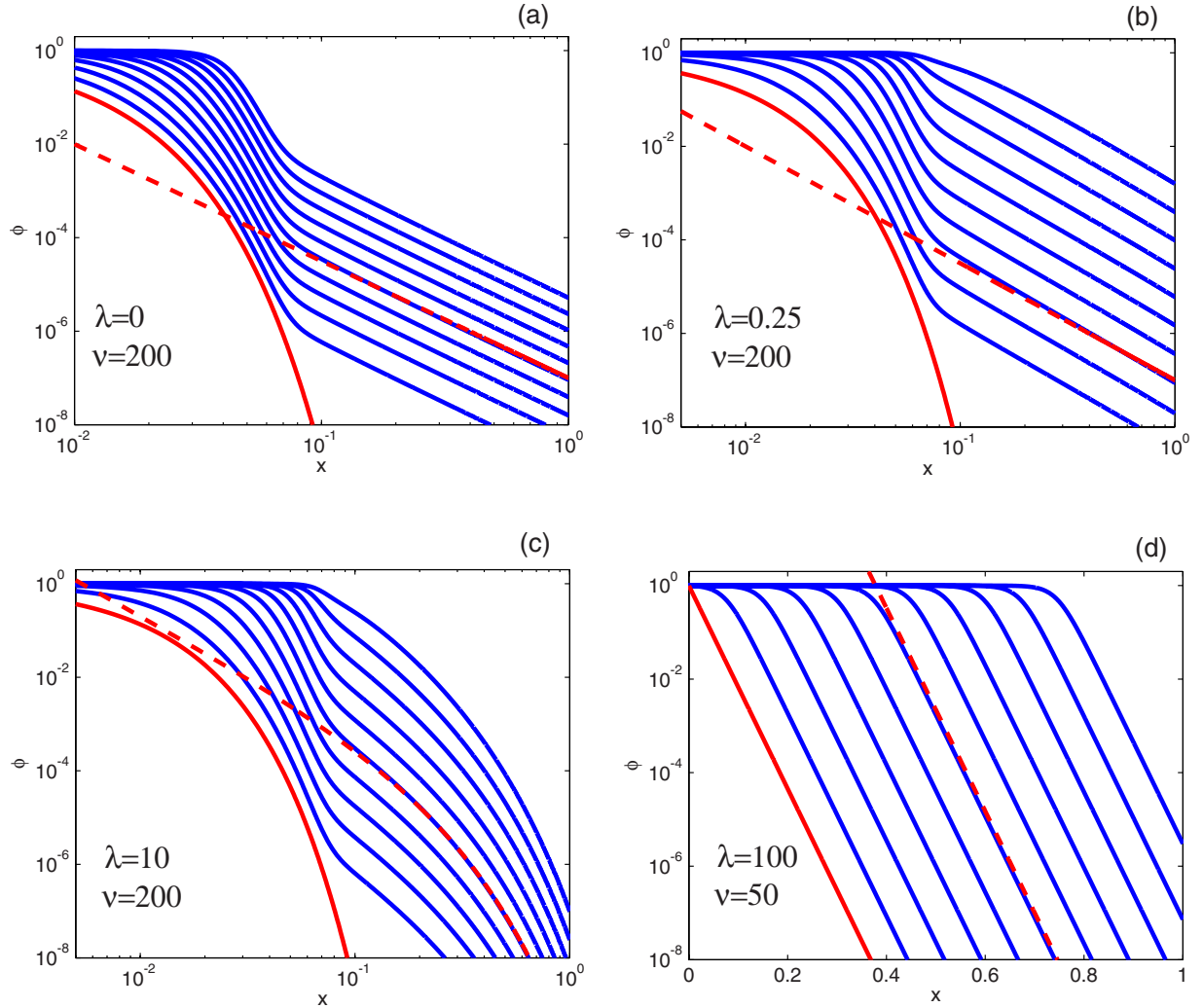


FIG. 2. (Color online) Depending on the value of the truncation parameter  $\lambda$ , four front propagation regimes can be distinguished in the truncated fractional Fisher-Kolmogorov Eq. (23). (a) Asymptotic algebraic regime for  $\lambda=0$ ; (b) intermediate asymptotic algebraic regime for  $\lambda \neq 0$ ; (c) truncated regime for  $0 < \lambda < \nu$ ; (d) overtruncated regime for  $\lambda > \nu$ . In all four panels the leftmost (red) curve denotes the initial condition in Eq. (24) and the other (blue) solid line curves show the front profiles at different times. The dashed (red) curve shows the analytical asymptotic result according to Eq. (36) with  $A=0$  in (a) and (b); according to Eq. (45) in (c); and according to Eq. (53) in (d). In all cases  $\alpha=1.5$ ,  $\theta=-1$ ,  $\gamma=1$ , and  $\chi=5 \times 10^{-7}$ .

of the Lagrangian velocity and acceleration. The solid line curves denote the numerical results for different values of  $\lambda$ . It is observed that the convergence to the terminal velocity scales as  $v_* - v_L \sim 1/t$  and the decay of the transient acceleration scales as  $a_L \sim 1/t^2$ . These numerical results are in agreement with the asymptotic scaling, shown with dashed line curves, which will be discussed in the following section.

#### IV. LEADING EDGE ASYMPTOTIC DYNAMICS: ANALYTICAL RESULTS

In this section we present analytical results describing the asymptotic behavior of fronts in the truncated fractional Fisher-Kolmogorov equation. The results are based on the leading edge approximation. This approximation exploits the idea that at the leading edge of the front  $\phi \ll 1$ , and therefore in this region the nonlinear reaction term can be linearized around  $\phi=0$ , resulting in the linear equation

$$\partial_t \phi = \chi e^{-\lambda x} {}_{-\infty} D_x^\alpha (e^{\lambda x} \phi) + (\gamma - \chi \lambda^\alpha) \phi. \quad (25)$$

Note that the truncated fractional derivative has a direct effect on the growth rate through the term  $-\chi \lambda^\alpha$ . As discussed in the previous section, this term is key to guarantee the conservation of the transported field. Two characteristic time scales can be distinguished in this problem: the time scale for the crossover to Gaussian statistics,  $\tau_c \sim 1/(\chi \lambda^\alpha)$ , and the reaction time scale,  $\tau_r = 1/\gamma$ . We will assume that  $\tau_c > \tau_r$  to guarantee that the effective reaction constant  $\gamma_{\text{eff}} = \gamma - \chi \lambda^\alpha$  is positive as needed for the excitation and propagation of “pull”-type fronts.

Substituting

$$\phi = e^{-\lambda x + (\gamma - \chi \lambda^\alpha)t} \psi(x, t) \quad (26)$$

into Eq. (25) gives the asymmetric,  $\alpha$ -stable fractional diffusion equation

$$\partial_t \psi = \chi {}_{-\infty} D_x^\alpha \psi. \quad (27)$$

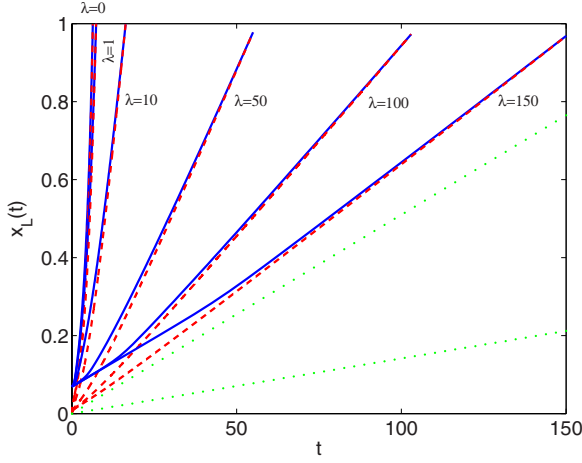


FIG. 3. (Color online) Space-time Lagrangian front paths,  $\phi(x_L(t), t) = \phi_0$  with  $\phi_0 = 10^{-6}$ , according to the asymmetric truncated fractional Fisher-Kolmogorov equation (23) with  $\alpha = 1.5$ ,  $\theta = -1$ ,  $\gamma = 1$ ,  $\chi = 5 \times 10^{-7}$ , and different values of  $\lambda$ . The solid (blue) curves denote the numerical results and the dashed (red) curves the asymptotic result according to Eq. (47). The dotted (green) lines denote the front speed (upper line) and the minimum front speed (lower line) in the Gaussian diffusive case according to Eq. (35). As the  $\lambda = 1$  case shows, the effect of truncation is negligible in the intermediate asymptotic regime.

The general solution of this equation for an initial condition  $\psi(x, t = 0) = \psi_0(x)$  can be written as

$$\psi(x, t) = \int_{-\infty}^{\infty} \hat{G}_{\alpha, 1, -1, 0}(\eta) \psi_0[x - (\chi t)^{1/\alpha} \eta] d\eta, \quad (28)$$

where  $\hat{G}_{\alpha, 1, -1, 0}$  is given in Eq. (18).

Consistent with the numerical simulations, we consider an initial condition of the form  $\phi(x, t = 0) = A$  for  $x < 0$  and  $\phi(x, t = 0) = e^{-\nu x}$ , where  $A$  and  $\nu$  are constants. Substituting the corresponding initial condition for  $\psi$ , according to Eq. (26), into the solution in Eq. (28) we get

$$\begin{aligned} \psi = & e^{-(\nu-\lambda)x} \int_{-\infty}^{x/\tau} e^{(\nu-\lambda)\tau\eta} \hat{G}_{\alpha, 1, -1, 0}(\eta) d\eta \\ & + A e^{\lambda x} \int_{x/\tau}^{\infty} \hat{G}_{\alpha, 1, -1, 0}(\eta) e^{-\lambda\tau\eta} d\eta, \end{aligned} \quad (29)$$

where we have defined  $\tau = (\chi t)^{1/\alpha}$ . In terms of  $\phi$  the solution can be written as

$$\phi = e^{-\nu x + (\gamma - \chi \lambda^\alpha)t} \mathcal{I}_1 + A e^{(\gamma - \chi \lambda^\alpha)t} \mathcal{I}_2, \quad (30)$$

where

$$\begin{aligned} \mathcal{I}_1 = & \int_{-\infty}^{x/\tau} e^{(\nu-\lambda)\tau\eta} \hat{G}_{\alpha, 1, -1, 0}(\eta) d\eta, \\ \mathcal{I}_2 = & \int_{x/\tau}^{\infty} \hat{G}_{\alpha, 1, -1, 0}(\eta) e^{-\lambda\tau\eta} d\eta. \end{aligned} \quad (31)$$

The goal of this section is to study the asymptotic behavior of  $\mathcal{I}_1$  and  $\mathcal{I}_2$  for  $x/\tau \rightarrow \infty$ . Before getting into the calculation

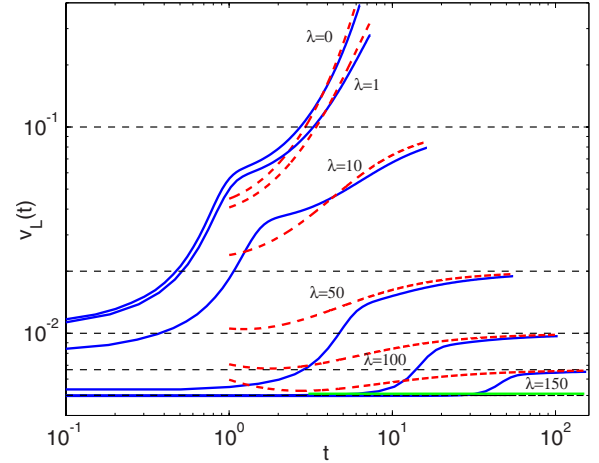


FIG. 4. (Color online) Time dependence of Lagrangian front velocities  $v_L(t) = dx_L(t)/dt$  according to the asymmetric truncated fractional Fisher-Kolmogorov equation (23) with  $\alpha = 1.5$ ,  $\theta = -1$ ,  $\gamma = 1$ ,  $\chi = 5 \times 10^{-7}$ , and different values of  $\lambda$ . The solid (blue) curves denote the numerical results and the dashed (red) curves the asymptotic result according to Eq. (48). The horizontal (black) dashed lines denote the corresponding terminal velocities according to Eq. (50). The solid (green) line at the bottom denotes the corresponding front speed in the Gaussian diffusive case according to Eq. (35).

of main interest here, it is instructive to consider first the diffusive (Gaussian) and fractional ( $\alpha$ -stable) limits of the leading edge solution in Eq. (30).

### A. Diffusive case

In the diffusive (Gaussian) case,  $(\alpha, \theta, \lambda) = (2, 0, 0)$ , the leading edge solution in Eq. (30) reduces to

$$\phi = e^{-\nu x + \gamma t} \int_{-\infty}^{x/\sqrt{\chi t}} \hat{G}_{2, 1, 0, 0}(\eta) e^{\nu \eta \sqrt{\chi t}} d\eta + A e^{\gamma t} \int_{x/\sqrt{\chi t}}^{\infty} \hat{G}_{2, 1, 0, 0} d\eta, \quad (32)$$

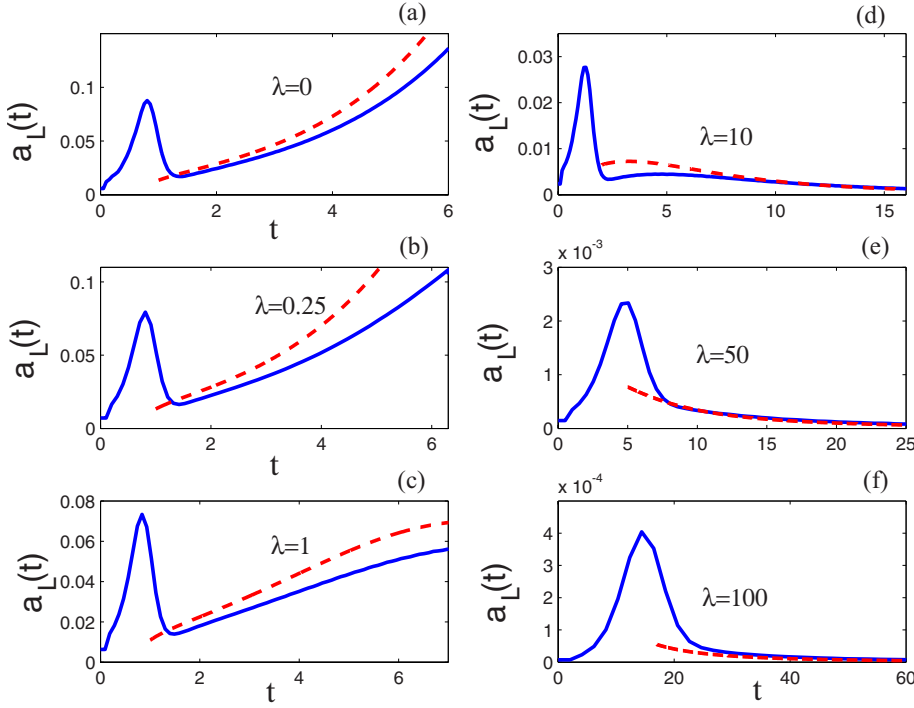
where  $\hat{G}_{2, 1, 0, 0} = 1/(2\sqrt{\pi}) e^{-\eta^2/4}$  is the Gaussian propagator. Introducing the normal probability distribution function  $P(z) = (1/\sqrt{2\pi}) \int_{-\infty}^z e^{-u^2/2} du$ ,

$$\phi = e^{-\nu x + (\gamma + \nu^2 \chi)t} P\left(\frac{x - 2\nu\chi t}{\sqrt{2\chi t}}\right) + A e^{\gamma t} \left[ 1 - P\left(\frac{x}{\sqrt{2\chi t}}\right) \right]. \quad (33)$$

Using the asymptotic expansion  $P(z) \sim 1 - (1/\sqrt{2\pi}) e^{-z^2/2}/z$ , we conclude that in the limit  $\eta = x/\tau \gg 1$ ,  $x > 2\nu\chi t$

$$\phi \sim e^{-\nu(x-ct)} + \sqrt{\frac{\chi t}{\pi}} \left( \frac{A}{x} - \frac{1}{x - 2\nu\chi t} \right) e^{-(\gamma/c_m^2 t)(x-c_m t)(x+c_m t)}, \quad (34)$$

where



$$c = \frac{\gamma}{\nu} + \nu\chi. \quad (35)$$

That is, in this case, the leading edge exhibits the well-known asymptotic exponential dependence,  $\phi \sim e^{-\nu(x-ct)}$ , and the front propagates at the constant speed  $c$  with  $c_m = 2\sqrt{\gamma\chi}$  corresponding to the minimum speed achieved for  $\nu = \sqrt{\gamma/\chi}$ . Note that according to Eq. (34) in this case the convergence to constant speed is exponentially fast, i.e., the second term in the asymptotic expansion scales as  $\sim e^{-a(x/\nu)^2}$ . This result will be contrasted below with the much slower convergence in the case of truncated Lévy flights.

### B. Fractional case

The fractional ( $\alpha$ -stable) case was discussed in Ref. [10]. In this case, the leading edge solution is given by Eqs. (30) and (31) with  $\lambda=0$  and the corresponding leading asymptotic behavior is

$$\phi \sim \chi t e^{\gamma} \left( \frac{A}{\alpha} x^{-\alpha} + \frac{1}{\nu} x^{-1-\alpha} + \dots \right), \quad (36)$$

where as mentioned before the constant  $A$  relates to the boundary condition  $\phi=A$  for  $x<0$ . The critical difference from the Gaussian case is the algebraic decay of the leading edge accompanied by the exponential acceleration of the

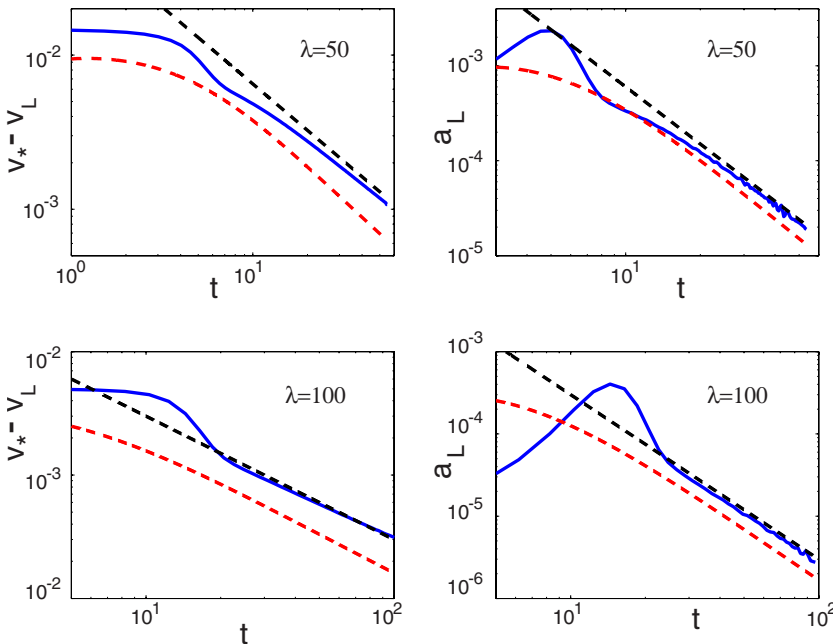


FIG. 6. (Color online) Asymptotic algebraic scaling of approach to terminal velocity  $v_* - v_L$ , and asymptotic algebraic scaling of Lagrangian front acceleration decay. The solid (blue) curves denote the numerical results for  $\alpha=1.5$ ,  $\theta=-1$ ,  $\gamma=1$ ,  $\chi=5 \times 10^{-7}$ , and different values of  $\lambda$ . The dashed (red) curves show the asymptotic results according to Eqs. (48) and (51), and the dashed (black) straight lines the analytical asymptotic scalings  $v_* - v_L \sim \alpha/(\lambda t)$  and  $a_L \sim \alpha/(\lambda t^2)$  according to Eqs. (49) and (52).

front. Note that when  $A \neq 0$  (which was the case considered in Ref. [10]) the front tail exhibits the decay  $\phi \sim 1/x^\alpha$ . However, when  $A=0$ , the front decays faster,  $\phi \sim 1/x^{\alpha+1}$ . Figure 2(a) shows a numerical verification of this scaling. This result will be contrasted with the truncated Lévy flight case, where, as in the Gaussian case, it will be shown that the rate of decay of the front's tail is independent of  $A$ .

In the Gaussian case, the spatiotemporal evolution of the leading edge depends to leading order on the variable  $x - ct$  which implies a ‘‘rigid’’ translation of the exponential tail of the front and allows the interpretation of  $c$  as the front. However, in the non-Gaussian case each point of the leading edge moves at a different speed and the tail does not translate rigidly. As discussed in the previous section we circumvent this problem by considering the Lagrangian trajectory  $x_L = x_L(t; \phi_0)$  of a point in the leading edge of the front such that  $\phi(x_L(t), t) = \phi_0$  where  $\phi_0 \ll 1$ . According to Eq. (36), in the  $\alpha$ -stable case, for  $A=0$ ,

$$x_L(t) = C \exp\left(\frac{1}{1 + \alpha}(\gamma t + \ln t)\right), \quad (37)$$

where  $C$  is a constant that depends on  $\phi_0$ ,  $\chi$ , and  $\nu$ , and

$$v_L(t) = \frac{\gamma}{1 + \alpha} \left(\frac{\chi t}{\phi_0 \nu}\right)^{1/(1+\alpha)} \left[\frac{1}{\gamma t} + 1\right] e^{[\gamma/(1+\alpha)]t}, \quad (38)$$

which implies an unbounded, exponential growth of the front speed. For large  $t$ , the corresponding leading-order behavior of the front acceleration is

$$a_L(t) = \left(\frac{\gamma}{1 + \alpha}\right)^2 \left(\frac{\chi t}{\phi_0 \nu}\right)^{1/(1+\alpha)} e^{[\gamma/(1+\alpha)]t}. \quad (39)$$

As shown in Figs. 3–5 the asymptotic results in Eqs. (37)–(39) are in good agreement with the numerical results discussed in the previous section.

### C. Truncated case

Going back to the general truncated fractional case, we consider first the asymptotic behavior of  $\mathcal{I}_2$  in Eq. (31). In the limit  $x/\tau \rightarrow \infty$ , the integration variable satisfies  $\eta \gg 1$  and thus we can use the asymptotic expression of the Green's function corresponding to the right, algebraically decaying tail,  $G_{\alpha,1,-1,0} \sim \eta^{-(1+\alpha)}$ , and get, after an integration by parts, the asymptotic expansion

$$\begin{aligned} \mathcal{I}_2 &\sim \int_{x/\tau}^{\infty} e^{-\lambda \tau \eta} \eta^{-(1+\alpha)} d\eta \\ &= \frac{\tau^\alpha e^{-\lambda x}}{\lambda x^{1+\alpha}} - \frac{\alpha + 1}{\lambda \tau} \int_{x/\tau}^{\infty} e^{-\lambda \tau \eta} \eta^{-(\alpha+2)} d\eta. \end{aligned} \quad (40)$$

Integration by parts once more gives the next term in the asymptotic series,

$$\mathcal{I}_2 \sim \frac{\tau^\alpha e^{-\lambda x}}{\lambda x^{1+\alpha}} \left(1 - \frac{(\alpha + 1)}{\lambda x} + \dots\right). \quad (41)$$

To deal with  $\mathcal{I}_1$ , introduce a cutoff  $\Omega$  such that  $1 \ll \Omega$  and write the integral as

$$\mathcal{I}_1 = C + \int_{\Omega}^{x/\tau} e^{(\nu-\lambda)\tau\eta} \hat{G}_{\alpha,1,-1,0}(\eta) d\eta, \quad (42)$$

where the constant on the right-hand side is defined as  $C = \int_{-\infty}^{\Omega} e^{(\nu-\lambda)\tau\eta} G_{\alpha,1,-1,0}(\eta) d\eta$ . Note that because of the faster than exponential decay of the asymmetric Lévy distribution  $G_{\alpha,1,-1,0}(\eta)$  for  $\eta < 0$  in Eq. (20) the integrals converge for either sign of  $\nu - \lambda$ . Since both the cutoff  $\Omega$  and  $x/\tau$  are assumed to be large, we can substitute as before the asymptotic expression of the Green's function in the integral of Eq. (42), and after an integration by parts obtain the asymptotic expansion

$$\mathcal{I}_1 \sim C + \frac{\tau^\alpha}{\nu - \lambda} \frac{e^{(\nu-\lambda)x}}{x^{1+\alpha}} + \dots \quad (43)$$

Substituting Eqs. (43) and (41) into Eq. (30) we get

$$\phi \sim C e^{-\nu x + (\gamma - \chi \lambda^\alpha)t} + \left(\frac{1}{\nu - \lambda} + \frac{A}{\lambda}\right) \frac{\chi t}{x^{\alpha+1}} e^{-\lambda x + (\gamma - \chi \lambda^\alpha)t} \quad (44)$$

for  $\nu \neq \lambda$ . The issue now is to determine the leading order term in Eq. (44). The answer to this problem depends on the relative values of  $\nu$  and  $\lambda$ .

If  $\nu > \lambda > 0$ , i.e., if the initial condition decays faster than the truncation, the leading order term in Eq. (44) for large  $x$  is

$$\phi \sim \left(\frac{1}{\nu - \lambda} + \frac{A}{\lambda}\right) \frac{t \chi}{x^{1+\alpha}} e^{-\lambda x + (\gamma - \chi \lambda^\alpha)t}. \quad (45)$$

Note that, contrary to the  $\alpha$ -stable case, the asymptotic spatial decay of the front leading edge in Eq. (45) is independent of the value of  $A$ . The role of the truncation is clearly seen in the exponential factor  $e^{-\lambda x}$  that dominates the decay for  $x \gg 1/\lambda$ . Figure 2(c) shows a very good agreement between the numerical result and the scaling in Eq. (45).

When  $x \ll 1/\lambda$  we can expand the exponential in Eq. (45) and write

$$\phi \sim \left(\frac{1}{\nu - \lambda} + \frac{A}{\lambda}\right) t \chi e^{(\gamma - \chi \lambda^\alpha)t} \frac{1}{x^{1+\alpha}} \left(1 - \lambda x + \frac{\lambda^2}{2} x^2 \dots\right). \quad (46)$$

According to Eq. (46) in the intermediate asymptotic regime  $(\chi t)^{1/\alpha} \ll x \ll 1/\lambda$ , the front exhibits to leading order the ideal (untruncated) Lévy flight algebraic scaling,  $\phi \sim 1/x^{1+\alpha}$ . This scaling is numerically verified in Fig. 2(b). Moreover, as Figs. 3–5 show, in the intermediate asymptotic regime (which in the numerical simulations roughly corresponds to  $0 < \lambda \leq 1$ ), the front's velocity and acceleration exhibit unbounded monotonic growth and follow to a good approximation the ideal Lévy flight scaling in Eqs. (37)–(39).

Going back to Eq. (45) we have that outside the intermediate asymptotic regime, i.e., for  $x > 1/\lambda$ , the Lagrangian trajectory of the front is given by

$$-\lambda x_L(t) + (\gamma - \chi \lambda^\alpha)t + \ln t - (\alpha + 1) \ln x_L(t) = M, \quad (47)$$

where  $M$  is a constant that depends on  $\phi_0$ . From Eq. (47) we obtain the following expression for the Lagrangian velocity of the front,  $v_L = dx_L(t)/dt$ :

$$v_L(t) = \frac{\gamma - \chi\lambda^\alpha + 1/t}{\lambda + (\alpha + 1)/x_L(t)}. \quad (48)$$

As shown in Figs. 3 and 4 there is good agreement between the numerical results (solid lines) and Eqs. (47) and (48) (dashed lines) in the asymptotic regime  $x \gg (\chi t)^{1/\alpha}$ . From Eq. (48) it follows that in the limit  $t \rightarrow \infty$

$$v_L \sim v_* - \frac{\alpha}{\lambda t} \dots, \quad (49)$$

where the terminal velocity is given by

$$v_* = \frac{\gamma - \lambda^\alpha \chi}{\lambda}, \quad (50)$$

which is positive since it has been assumed that  $\gamma > \lambda^\alpha \chi$ . The asymptotic approach to the terminal velocity is clearly observed in Fig. 4 where the horizontal dashed lines show the terminal velocity in Eq. (50) for the values of  $\lambda$  considered in the numerical simulations. According to Eq. (49) the time required for the front velocity to approach the terminal velocity within a given margin  $v_* - v_L$  scales as  $t \sim 1/\lambda$ . The corresponding Lagrangian acceleration of the front,  $a_L = dv_L(t)/dt$ , is given by

$$a_L(t) = \frac{v_L(t)}{t(\lambda t v_* + 1)} \left[ (\alpha + 1) \left( \frac{v_L(t)}{x_L(t)/t} \right)^2 - 1 \right]. \quad (51)$$

From Eqs. (48) and (51) it follows that for large times

$$a_L(t) \sim \frac{\alpha}{\lambda t^2}. \quad (52)$$

As shown in Fig. 6, the analytical scaling relations agree well with the numerical results. In this figure, the curved dashed lines correspond to the analytical result in Eqs. (48) and (51) and the straight dashed lines correspond to the scaling in Eqs. (50) and (52). Thus, outside the intermediate asymptotic regime, i.e., for  $1/\lambda < x$ , the front acceleration decays and the front approaches a constant terminal velocity as  $t \rightarrow \infty$ . However, the convergence of the dynamics to the constant front velocity regimen exhibits a very slow,  $\sim 1/(\lambda t)$ , algebraic decay compared to the significantly faster exponential convergence in the diffusive case.

The calculations presented up to now assumed  $\nu > \lambda$ . However, when  $\lambda > \nu$ , i.e., when the initial condition decays more slowly than the truncation, the leading order term in Eq. (44) is

$$\phi \sim C e^{-\nu x + (\gamma - \lambda^\alpha \chi)t}, \quad (53)$$

which indicates that the front moves with the constant velocity

$$v = \frac{\gamma - \lambda^\alpha \chi}{\nu}. \quad (54)$$

An example of this overtruncated regime is presented in Fig. 2(d), which shows a very good agreement with the exponential decay in Eq. (53) for  $\lambda=100$  and  $\nu=50$ . The remaining case to consider is  $\lambda = \nu$ . In this case, the asymptotic approximation in Eq. (41) still holds. However, the expression in Eq.

(43) cannot be used, and we have to go back to the integral  $\mathcal{I}_1$  Eq. (42),

$$\mathcal{I}_1 = C + \int_{\Omega}^{x/\tau} G_{\alpha,1,-1,0}(\eta) d\eta, \quad (55)$$

where this time the constant on the right-hand side is defined as  $C = \int_{-\infty}^{\Omega} \hat{G}_{\alpha,1,-1,0}(\eta) d\eta$ . Using the asymptotic expression for  $\hat{G}_{\alpha,1,-1,0} \sim \eta^{-1-\alpha}$  and integrating, it is concluded that the leading order term in Eq. (30) is  $\phi \sim C e^{-\lambda x + (\gamma - \lambda^\alpha \chi)t}$ , which implies that the constant velocity of the front is given by Eq. (54) with  $\nu = \lambda$ .

## V. CONCLUSIONS

We have presented a numerical and analytical study of the role of truncated Lévy flights in the propagation of fronts in reaction superdiffusion systems. The study was based on the truncated fractional Fisher-Kolmogorov model in which the spatial derivative is replaced by the  $\lambda$ -truncated fractional derivative of order  $\alpha$ .

Depending on the level of truncation four front propagation regimes can be distinguished: an asymptotic algebraic regime, an intermediate asymptotic algebraic regime, a truncated regime, and an overtruncated regime. The asymptotic algebraic regime corresponds to  $\lambda=0$ . In this case the problem reduces to the  $\alpha$ -stable fractional Fisher-Kolmogorov problem which exhibits exponential acceleration and algebraically decaying tails for  $x \gg (\chi t)^{1/\alpha}$ . The intermediate asymptotic regime is characterized by  $(\chi t)^{1/\alpha} \ll x \ll 1/\lambda$ . We have shown numerically and analytically that in this regime the truncation effects are negligible and the algebraic decay of the tail as well as the acceleration of the front prevail. Outside the intermediate asymptotic regime, i.e., for  $x > 1/\lambda$  and  $(\chi t)^{1/\alpha} \ll x$ , the tail of the front exhibits the tempered decay  $\phi \sim e^{-\lambda x}/x^{1+\alpha}$ , the acceleration is transient, and the front eventually reaches a terminal speed as  $t \rightarrow \infty$ . In the overtruncated regime the truncation decays faster than the initial condition, i.e.,  $\lambda > \nu$ . In this case, Lévy flights have apparently no qualitative effect on the asymptotic dynamics of the front that exhibits a diffusive-type exponential tail,  $\phi \sim e^{-\nu x}$ , and constant propagation velocity  $v = \gamma_{\text{eff}}/\nu$ . However, contrary to the diffusive case, the constant velocity in the overtruncated case is a monotonically decaying function of  $\nu$  and has no finite minimum.

Although in the truncated regime the acceleration decays and the front eventually reaches a constant terminal speed, the numerical and analytical results show that the convergence of this process is very slow. In particular the front acceleration asymptotically decays as  $a_L \sim \alpha/(\lambda t^2)$  and the approach to the terminal velocity scales as  $v_L \sim v_* - \alpha/(\lambda t)$ . This algebraic convergence is in sharp contrast with the exponential convergence observed in the diffusive Fisher-Kolmogorov equation. In this sense the truncated regime resembles the ‘‘ultraslow’’ convergence regimen observed in transport problems without reaction terms.

One of the motivations and potential applications of the present work lays on the study of transport in magnetically confined plasmas. In this system it has been suggested that

reaction diffusion models provide insightful, though highly simplified, reduced descriptions of the interaction of turbulence and transport. Current models usually assume Laplacian diffusive operators; see, for example, Ref. [31]. However, there is evidence that transport in magnetically confined plasmas is not necessarily diffusive; see, for example, [32], and references therein. On the other hand, it has been argued that truncated Lévy distributions might play a role in the description of electrostatic potential fluctuations [33]. Based on this, it would be of interest to explore the implications of the present work for the corresponding plasma transport models.

Throughout this paper we have limited attention to extremal,  $\theta=-1$ , transport processes and assumed an external advection velocity to cancel the drift resulting from the truncation of the asymmetric fractional derivative. A problem of interest is to perform more general numerical simulations considering different degrees of asymmetry and including memory effects through the use of fractional derivatives in

time. As mentioned in the Introduction, in recent years several papers have discussed the role of Lévy flights in front propagation and pattern formation in reaction–anomalous-diffusion systems. It would be of interest to explore the role of truncation effects in these systems. Beyond its intrinsic theoretical interest, the study presented here might have relevance in the interpretation and modeling of laboratory experiments and numerical simulations of complex systems. It is plausible that in these systems, the presence of boundary conditions, finite size domain and decorrelation could introduce nonideal Lévy flight dynamics of the type discussed here.

#### ACKNOWLEDGMENTS

This work has been supported by the Oak Ridge National Laboratory, managed by UT-Battelle, LLC, for the U.S. Department of Energy under Contract No. DE-AC05-00OR22725.

- 
- [1] M. C. Cross and P. C. Hohenberg, *Rev. Mod. Phys.* **65**, 851 (1993).
  - [2] J. D. Murray, *Mathematical Biology* (Springer-Verlag, New York, 1989).
  - [3] R. Metzler and J. Klafter, *J. Phys. A* **37**, R161 (2004).
  - [4] J. P. Bouchaud and A. Georges, *Phys. Rep.* **195**, 127 (1990).
  - [5] *Anomalous Transport. Foundations and Applications*, edited by R. Klages, G. Radons, and I. M. Sokolov (Wiley-VCH Verlag, Weinheim, 2008).
  - [6] R. Metzler and J. Klafter, *Phys. Rep.* **339**, 1 (2000).
  - [7] D. H. Zanette, *Phys. Rev. E* **55**, 1181 (1997).
  - [8] B. I. Henry and S. L. Wearne, *Physica A* **276**, 448 (2000).
  - [9] R. Mancinelli, D. Vergni, and A. Vulpiani, *Europhys. Lett.* **60**, 532 (2002).
  - [10] D. del-Castillo-Negrete, B. A. Carreras, and V. E. Lynch, *Phys. Rev. Lett.* **91**, 018302 (2003).
  - [11] A. Torcini and S. Lepri, *Phys. Rev. E* **55**, R3805 (1997).
  - [12] R. K. Saxena, A. M. Mathai, and H. J. Haubold, *Astrophys. Space Sci.* **305**, 289 (2006).
  - [13] D. Hernandez, R. Barrio, and C. Varea, *Phys. Rev. E* **74**, 046116 (2006).
  - [14] I. M. Sokolov, M. G. W. Schmidt, and F. Sagues, *Phys. Rev. E* **73**, 031102 (2006).
  - [15] D. Brockmann and L. Hufnagel, *Phys. Rev. Lett.* **98**, 178301 (2007).
  - [16] T. A. M. Langlands, B. I. Henry, and S. L. Wearne, *J. Phys.: Condens. Matter* **19**, 065115 (2007).
  - [17] A. A. Golovin, B. J. Matkowsky, and V. A. Volpert, *SIAM J. Appl. Math.* **69**, 251 (2008).
  - [18] Y. Nec, A. A. Nepomnyashchy, and A. A. Golovin, *Europhys. Lett.* **82**, 58003 (2008).
  - [19] R. N. Mantegna and H. E. Stanley, *Phys. Rev. Lett.* **73**, 2946 (1994).
  - [20] I. Koponen, *Phys. Rev. E* **52**, 1197 (1995).
  - [21] W. Feller, *An Introduction to Probability Theory and Its Applications* (Wiley, New York, 1966), Vol. 2, Chap. XVI.8, p. 525.
  - [22] M. F. Shlesinger, *Phys. Rev. Lett.* **74**, 4959 (1995).
  - [23] A. Cartea and D. del-Castillo-Negrete, *Phys. Rev. E* **76**, 041105 (2007).
  - [24] I. M. Sokolov, A. V. Chechkin, and J. Klafter, *Physica A* **336**, 245 (2004).
  - [25] I. Podlubny, *Fractional Differential Equations* (Academic, San Diego, 1999).
  - [26] S. G. Samko, A. A. Kilbas, and O. I. Marichev, *Fractional Integrals and Derivatives* (Gordon and Breach, Amsterdam, 1993).
  - [27] G. Samorodnitsky and M. S. Taqqu, *Stable Non-Gaussian Random Processes* (Chapman & Hall, New York, 1994).
  - [28] F. Mainardi, Y. Luchko, and G. Pagnini, *Fractional Calculus Appl. Anal.* **4**, 153 (2001).
  - [29] D. del-Castillo-Negrete, *Phys. Plasmas* **13**, 082308 (2006).
  - [30] V. Lynch, B. A. Carreras, D. del-Castillo-Negrete, K. M. Ferreira-Mejias, and H. R. Hicks, *J. Comput. Phys.* **192**, 406 (2003).
  - [31] D. del-Castillo-Negrete and B. A. Carreras, *Phys. Plasmas* **9**, 118 (2002); X. Garbet, Y. Sarazin, F. Imbeaux, P. Ghendrih, C. Bourdelle, O. D. Gurcan, and P. H. Diamond, *ibid.* **14**, 122305 (2007).
  - [32] D. del-Castillo-Negrete, in *Turbulent Transport in Fusion Plasmas: First ITER International Summer School*, edited by S. Benkadda, AIP Conf. Proc. No. 1013 (AIP, Melville, NY, 2008).
  - [33] R. Jha, P. K. Kaw, D. R. Kulkarni, J. C. Parikh, and the ADITYA Team, *Phys. Plasmas* **10**, 699 (2003).